Nonrigid Shape Recovery by Gaussian Process Regression

Jianke Zhu
ETH Zurich
Switzerland
zhu@vision.ee.ethz.ch

Steven C.H. Hoi
Nanyang Tech. University
Singapore
chhoi@ntu.edu.sg

Michael R. Lyu
Chinese University of Hong Kong
Hong Kong
lyu@cse.cuhk.edu.hk

Abstract

Most state-of-the-art nonrigid shape recovery methods usually use explicit deformable mesh models to regularize surface deformation and constrain the search space. These triangulated mesh models heavily relying on the quadratic regularization term are difficult to accurately capture large deformations, such as severe bending. In this paper, we propose a novel Gaussian process regression approach to the nonrigid shape recovery problem, which does not require to involve a predefined triangulated mesh model. By taking advantage of our novel Gaussian process regression formulation together with a robust coarse-to-fine optimization scheme, the proposed method is fully automatic and is able to handle large deformations and outliers. We conducted a set of extensive experiments for performance evaluation in various environments. Encouraging experimental results show that our proposed approach is both effective and robust to nonrigid shape recovery with large deformations.

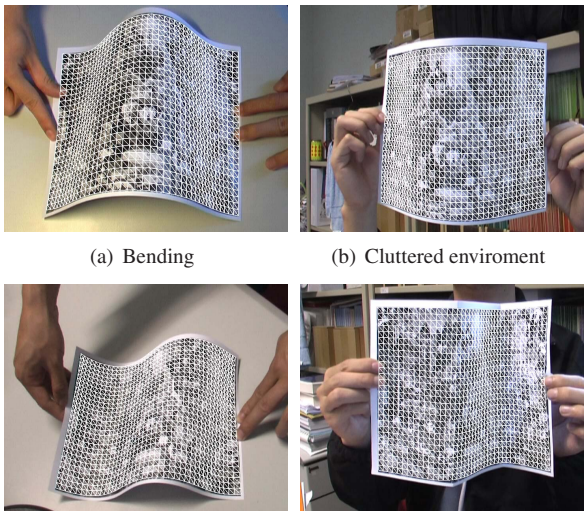

(a) Bending (b) Cluttered enviroment (c) Waveform (d) Sharply folded surface

Figure 1. Recovering highly deformable shapes from single image (a-d). (a) Severely bending. (b) Bended paper in clutter environment. (c) Waveform deformation. (d) Sharply folded paper.

1. Introduction

Nonrigid shape recovery [2, 16] in a visual scene is an important computer vision problem, which plays a critical role for a variety of applications in image analysis, medical imaging, augmented reality, digital entertainment and human computer interaction. Extensive research efforts in image analysis and computer vision domains have focused on the problems related to deformable object modeling and tracking [4, 16]. Such research work on deformable object tracking is closely related to problems such as image registration, feature matching, and object recognition.

In general, nonrigid shape recovery can be formulated as a problem of fitting a mapping function between a target model and some observations. Due to noisy observations, practical nonrigid shape recovery methods often require some effective solutions to reject non-homologies matchings. To this purpose, regularized deformable models are often engaged, which have been shown as a vital tool for handling noisy observation and ill-posed optimization.

Various regularization methods have been proposed, such as Thin-Plate Spline [21], data embedding methods, and Finite Element Models (FEM) [8, 16, 24, 25]. Thin-Plate Spline is a well-known interpolation method widely used in point set registration, which mainly penalizes the second order derivatives [21]. Besides, the data embedding techniques, such as Principal Component Analysis (PCA) [2, 20, 22], are also engaged as the regularization technique, although PCA requires a large number of training samples to obtain sufficient generalization capability. Finally, the FEM based regularization approach has also been extensively studied [8, 16, 25]. However, for the techniques using the FEM models, the nonrigid surface must be explicitly represented by a triangulated mesh. Moreover, the triangulated FEM models heavily rely on a quadratic regularization term, which usually limits their capability of accurately recovering sharply-folded and severely-bended surfaces, as shown in Fig. 1.

978-1-4244-3991-1/09/$25.00 ©2009 IEEE

Recently there are a surge of research interests on the 3D deformable surface tracking [18, 23]. These methods do not impose strong prior models, and often achieve considerably more accurate results. However, they often rely on either temporal information or certain good initialization in order to solve the ambiguity in the nonrigid surface recovery problem. Although some recent extension work of constraints-based methods in [19] avoids the initialization, their approach still needs 2D nonrigid surface detection techniques [16, 24, 25] in order to first reject large outliers.

Since all the existing approaches have limitations, there is a need for developing new techniques to resolve these challenges. In this paper, we attempt to solve the problem by proposing a novel Gaussian process regression approach for the nonrigid shape recovery. Gaussian processes [17] enjoy a solid foundation in statistics and machine learning, which provide a promising non-parametric Bayesian approach to regression problems and offer probability predictions. In contrast to the FEM-based nonrigid surface detection methods [16, 24, 25], the proposed Gaussian process approach does not require any explicit triangulated mesh representation for nonrigid shape model, and can handle large deformations without resorting to the 3D deformable surface model. Moreover, our proposed approach is fully automatic, which can recover the nonrigid shapes from cluttered environment. Fig. 1 illustrates the example results on severely-bended and sharply-folded surfaces.

The rest of this paper is organized as follows. Section 2 reviews some previous approaches related to nonrigid shape recovery. Section 3 proposes a novel Gaussian process regression approach to tackle the nonrigid shape recovery problem, and presents a practically-efficient optimization method using an effective active set selection scheme. Section 4 describes the details of our experimental implementation and discusses experimental results. Section 5 addresses limitations of our work and some future work. Section 6 sets out our conclusion.

2. Related Work

Considerable research efforts have been expended on the nonrigid shape modeling and recovery in image analysis and computer vision community [1, 16]. The methods presented in [16, 24] are designed to estimate mapping functions from some matched point pairs, which offer fully automatic solutions to detect and recover nonrigid surfaces. The correspondences are often built via some sophisticated feature matching algorithms, such as SIFT [11]. Ideally if the point correspondences contain no outliers, finding the nonrigid mapping function only requires solving simple linear equations. In practice, such ideal case seldom happens in a real computer vision problem, in which outliers could account for up to 90% of the points in some typical point matching problems [16]. Therefore, it is difficult to directly apply regular function estimation techniques widely used in statistics. This is because a typical statistical estimator requires that inliers must be the absolute majority of the data in order to achieve a reasonable solution [12].

Another group of research is based on the nonrigid point set matching, which intends to establish a consistent correspondence between two point sets and recover the mapping function with the best alignment. Extensive studies can be found in the literature [1, 13]. Rangaranjan et al. [4] present a coarse-to-fine approach to jointly determine the correspondences and nonrigid transformation between two point sets through deterministic annealing and soft-assign. The probabilistic approach for the nonrigid point set matching has attracted increasing research interests [9, 13]. The point set matching is interpreted as a mixture density estimation problem [7], where one point set represents the centers of Gaussian mixture models and the other represents sample data. Another idea is to model each of the two point sets by a kernel density function [9] and then measure the similarity. All these methods employ the Thin-Plate Spline to obtain smooth nonlinear transformation. Myroneko et al. [13] present a coherent point drift method for nonrigid point set registration, which does not make an explicit assumption on the transformation model.

In comparison to some real-time automated solution in [16], the point set matching methods [1, 13] are usually computationally very expensive, and few of them can be applied to point sets extracted from real images. In contrast, the feature correspondence based approaches have already been applied to track nonrigid objects in realtime videos.

Most recently, 3D deformable surface recovery has attracted increasing research interests in computer vision community. To address the highly ill-posed optimization problems, both temporal information and edge constraints [18, 23] are employed to constrain the surface deformation. However, these methods still rely on 2D nonrigid surface detection techniques in order to build reliable correspondences containing smaller noisy matches.

In this paper, we propose a novel fully automatic nonrigid shape recovery approach, which can effectively handle large deformations without resorting to a 3D environment. The key of our presented method is to formulate the nonrigid shape recovery as a Gaussian process regression task, which only makes the Gaussian process prior assumption on the nonrigid shape mapping. To the best of our knowledge, no existing study directly formulates the nonrigid shape recovery problem as a Gaussian process regression task.

3. Gaussian Process Regression Approach

In this section, we present the proposed Gaussian process regression approach to nonrigid shape recovery. We first formulate the nonrigid shape recovery problem as a Gaus-

sian process regression task. Then, we propose a practically efficient algorithm with an active set selection scheme to address the challenge of noisy observations. Finally, we present the details of our optimization approach.

3.1. Gaussian Process Regression Formulation

Let us denote by I_m and I_t the model image and the target image, respectively, $\mathbf{x}_i$ the 2D coordinates of a feature point in the model image I_m, and $\mathbf{y}_i$ the coordinates of its match in the target image I_t. Assume that a set of correspondences $M = \{(\mathbf{x}_i, \mathbf{y}_i) \in \mathbb{R}^d\}_{i=1}^n$ between the model and target images can be obtained through a point matching algorithm such as SIFT [11], where $d = 2$ and n is the total number of matched pairs.

The goal of nonrigid shape recovery is to find a latent function $f(\mathbf{x})$ to map the points in the model space into the target image space I_t. Mathematically, this can be formulated as a regression problem, which aims to fit a function from the input data of correspondence pairs $(\mathbf{x}, \mathbf{y})$. Let vector $\mathbf{y}$ denote the measurement target of the input vector $\mathbf{x}$. Typically, one can assume that the observed target data $\mathbf{y}$ differs from the function value $\mathbf{x}$ by some additive Gaussian noise $\boldsymbol{\epsilon}$ with zero mean and variance σ^2. Therefore, the target value can be written as $\mathbf{y} = f(\mathbf{x}) + \boldsymbol{\epsilon}$.

Following a Bayesian approach to regression, the posterior distribution over these latent functions f is derived below:

$$p(f|M) \propto p(f)p(M|f)$$

where the likelihood $p(M|f)$ captures how function values and observed data are related. $p(f)$ is the a priori probability of the random field $f(\mathbf{x})$, which embodies a priori knowledge to constrain the nonrigid shape model. Since a Gaussian process [17] is completely specified by its mean function $m(\mathbf{x})$ and covariance function $k(\mathbf{x}, \mathbf{x}')$, we write the Gaussian process posterior distribution over function $f(\mathbf{x})$ as follows:

$$p(f|M) \propto \mathcal{N}(f|m(\mathbf{x}), k(\mathbf{x}, \mathbf{x}')) \prod_{i=1}^{n} p_i(\mathbf{y}_i|f(\mathbf{x})) \quad (1)$$

where we define a nonrigid mapping function $f(\mathbf{x})$ as a Gaussian Process with the deterministic mean function $m(\mathbf{x}) = \mathbf{x}$:

$$f(\mathbf{x}) \sim \mathcal{GP}(\mathbf{x}, k(\mathbf{x}, \mathbf{x}')) \quad (2)$$

As discussed in [17], there are various choices for selecting the covariance function $k(\mathbf{x}, \mathbf{x}')$, such as linear, polynomial, exponential and rational quadratic, amongst others. We choose the squared exponential covariance function k:

$$k(\mathbf{x}, \mathbf{x}') = \exp\left(-\frac{1}{2\rho^2}\|\mathbf{x} - \mathbf{x}'\|^2\right)$$

Note that applying the mean function $m(\mathbf{x}) = \mathbf{x}$ is equivalent to employing the usual zero mean Gaussian process to model the difference between the observations and the mean function. Therefore, we can write the joint distribution of the observed target values $Y \in R^{n\times d}$ and the estimated function values $\mathbf{f}_*$ under the prior as:

$$\begin{bmatrix} \mathbf{Y} \\ \mathbf{f}_* \end{bmatrix} \propto \mathcal{N}\left(X, \begin{bmatrix} K_{X,X} + \sigma^2 I & K_{X,X_*} \\ K_{X_*,X} & K_{X_*,X_*} \end{bmatrix}\right)$$

where K is the covariance matrix, $X \in R^{n\times d}$ is the matrix of model points, and X_* denotes the points sampled from the model image. Thus, we can write the mean prediction matrix $\mathbf{f}^*(X)$ as follows:

$$\mathbf{f}^*(X_*) = X_* + K_{X_*,X}(K_{X,X} + \sigma^2 I)^{-1}(Y - X) \quad (3)$$

Using the compact notation for a single sampled point $\mathbf{x}$, the mean prediction of the mapping function $f^*(\mathbf{x})$ can be further written as follows:

$$f^*(\mathbf{x}) = \mathbf{x} + \mathbf{k}_*^\top (K + \sigma^2 I)^{-1}(Y - X) \quad (4)$$

where $\mathbf{k}_*^\top$ denotes the vector of covariances between the sampled model point and the n points in the model image. It can be further formulated as a linear combination of n kernel functions:

$$f^*(\mathbf{x}) = \mathbf{x} + \sum_{i=1}^{n} \boldsymbol{\alpha}_i k(\mathbf{x}, \mathbf{x}_i) \quad (5)$$

where $\boldsymbol{\alpha}_i$ is a d-dimensional coefficient vector. The optimal coefficient matrix $\boldsymbol{\alpha}$ can be computed by:

$$\boldsymbol{\alpha} = (K + \sigma^2 I)^{-1}(Y - X) \quad (6)$$

3.2. Nonrigid Shape Recovery

In general, incorrect matches cannot be avoided in the first stage of the feature matching process when only local image descriptors are compared. The great challenge for nonrigid shape recovery is to deal with large numbers of outliers. In this paper, we present a robust optimization scheme to attack this critical problem.

Since large outliers are overemphasized in the Gaussian process regression, we employ an active set selection scheme [10] to choose inlier matches. This approach chooses the inlier matches with estimated residual error $\delta = \mathbf{y} - f^*(\mathbf{x})$ below the variance σ, which is proven to be relatively insensitive to the outliers [3, 16, 24]. Therefore, we can obtain the following solution:

$$\boldsymbol{\alpha} = \left(I^0 K + \sigma^2 I\right)^{-1} \left[I^0 (Y - X)\right] \quad (7)$$

where I^0 denotes an $n \times n$ matrix with inliers' entries being one and others zero. Let $K' \in R^{l\times l}$ denote the matrix part

of the inliers block in the original kernel matrix K, and l is the number of inlier matches. Since l is always less than n, the above linear system in Eqn. 7 can be reduced to a smaller problem:

$$\boldsymbol{\alpha}' = \left(K' + \sigma^2 I\right)^{-1} \left(Y' - X'\right) \tag{8}$$

where Y' and X' refer to the inliers block of the corresponding matrices. $\boldsymbol{\alpha}'$ is an $l \times d$ matrix, which is associated with the inlier model points only. The above linear system can be efficiently solved by LU decomposition. Moreover, it can be observed that the outliers are not involved into the computation. In addition, both precision and computational cost of our method are dependent only on the total number of inlier points.

Furthermore, we introduce a weight ω_i associated with each feature correspondence. Similar to the one defined in EM-ICP [6], ω_i is the posterior probability, which decays exponentially as a function of distance, so that the large numbers of outliers have little influence on the minimization:

$$\omega_i = \frac{\exp(-\frac{1}{2\sigma^2} \left\| \mathbf{y}_i - f^*(\mathbf{x}_i) \right\|^2)}{\sum_{i=1}^{n} \exp(-\frac{1}{2\sigma^2} \left\| \mathbf{y}_i - f^*(\mathbf{x}_i) \right\|^2)}$$

Let W denote a diagonal weight matrix with $W_{ii} = \omega_i$, we can obtain the following solution:

$$\boldsymbol{\alpha}' = \left(W'K' + \sigma^2 \lambda I\right)^{-1} \left[W'(Y' - X')\right] \tag{9}$$

Note that a feature point in the model image I_m may be matched with multiple points in the target image I_t. Simply summing them together is equivalent to matching with the center of these points in I_t, which may be neither effective nor efficient. In this case, we only retain the correspondences with the highest match scores.

Once the mapping function $f^*(\mathbf{x})$ is computed, then we can warp the model image I_m to the target image I_t using Eqn. 5 for applications.

3.3. Optimization

In order to facilitate Gaussian process regression, we first normalize both the model and the target point sets with zero mean and unit variance. This procedure is equivalent to translating the central of the point set to the origin and scaling the point set size to one.

To handle the large numbers of outliers, we introduce an incremental outlier threshold scheme, which has been successfully used in [16, 24]. The noise variance σ is progressively decayed at a constant annealing rate γ, which means more feature correspondences will be selected as inliers with large noise variance. Moreover, the fitting results become more accurate when the noise variance becomes smaller. In order to select most of the correspondences into the initial active set, and to avoid getting stuck at local minima, the initial value of σ is usually set to a sufficiently large value. In our experiments, we set this value to 2 empirically.

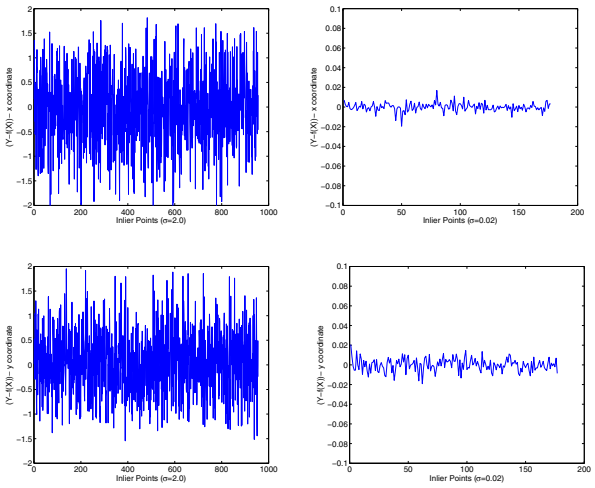

(a) $\sigma = 2$ (b) $\sigma = 0.02$

Figure 2. (a) $Y - \mathbf{f}(X)$ with 955 inlier matches when $\sigma = 2.0$. (b) $Y - \mathbf{f}(X)$ with 182 inlier matches when $\sigma = 0.2$.

For each value of σ, we estimate the mapping function through Eqn. 9 until the inlier set no longer changes or the maximum number of iterations is reached. The result is then employed as the initial state for the next minimization. Also, the inlier set is updated using the current estimated mapping function. To deal with the global transformation, we re-normalize the input point set with respect to the inliers for each noise variance level. The whole optimization procedure stops when noise variance σ reaches a value close to the expected precision, and then the algorithm reports a successful result when the number of inlier matches is above a given threshold. Ultimately, the proposed optimization scheme involves 2 or 3 iterations for each σ, and around 20 iterations in total to ensure the convergence. Fig. 2 plots the initial inlier $Y - \mathbf{f}(X)$ and the final results. We find that the magnitude of $Y - \mathbf{f}(X)$ is greatly reduced via the proposed optimization scheme.

3.4. Fast Computation

Since the optimization procedure only involves the part of the covariance matrix K that is constant in the whole process, we can pre-compute it to save computational cost. Similarly, we can pre-compute the projection matrix which maps the mesh from the model to the target.

In our experiments, we find that the registration accuracy can be guaranteed when reaching a sufficiently large number of inlier matches. On the other hand, too large number of inlier matches in the early optimization stage will incur heavy computational cost. Therefore, we select a suffi-

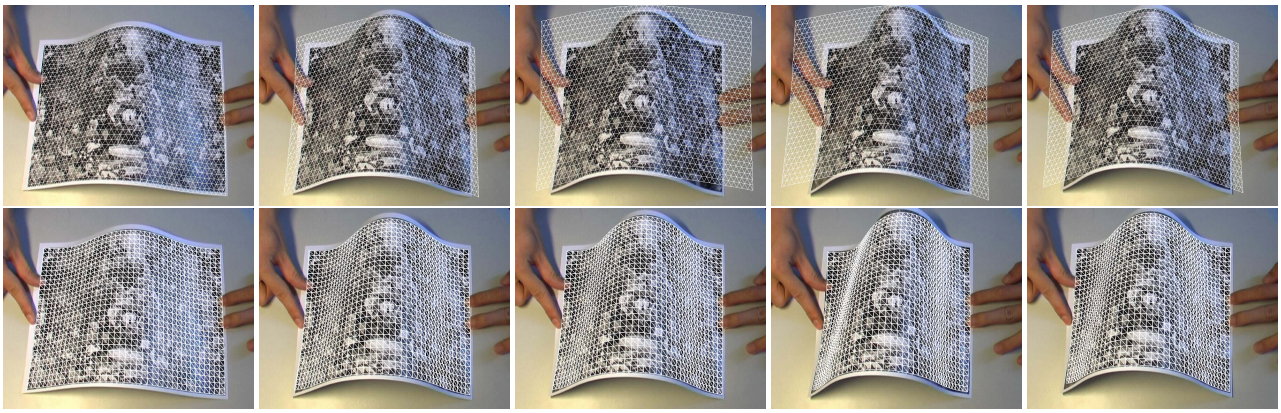

Figure 3. We use a piece of paper as the nonrigid surface. The first row shows the images captured by a DV camera size of 720×576 overlaid by the nonrigid shape recovery results using the FEM-based method [24]. The second row is our results for recovering the severely bended paper surface.

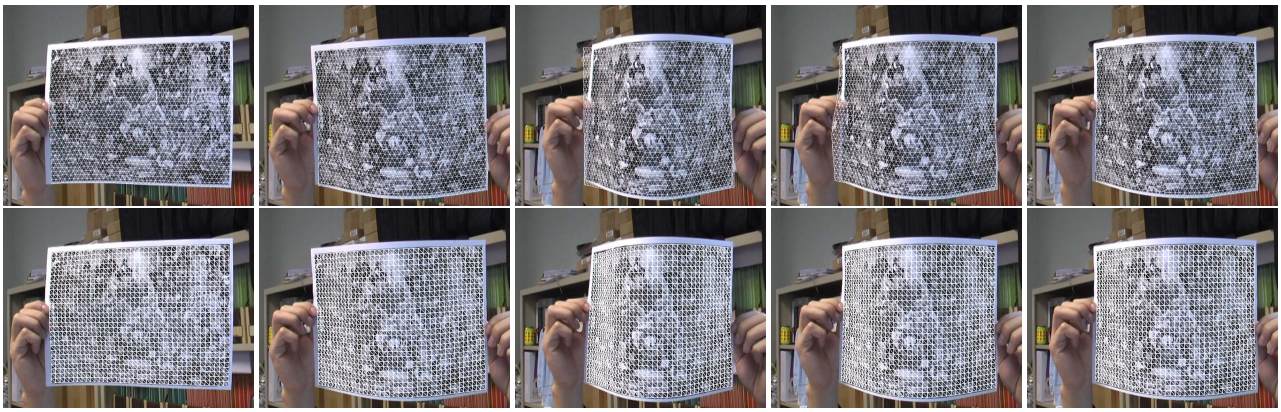

Figure 4. Recovering the bended paper surface in the cluttered environment. The first row shows the results using the FEM-based method [24]. The second row plots the results obtained from proposed method.

ciently large number of inlier matches when computing the mapping function to balance the tradeoff between accuracy and efficiency. In addition, instead of using a random sampling process, we employ the top ranked correspondences according to the feature matching scores, which is proven to be effective in pose estimation [5].

4. Experimental Results

In this section, we present the details of our experimental implementation and report the results of performance evaluation on nonrigid shape recovery. We demonstrate that the proposed approach is effective to handle large deformations in nonrigid shape recovery. In addition, similarly convincing results are obtained for medical image registration and 3D face alignment.

4.1. Experimental Setup

All the experiments reported in this paper were carried out on a Pentium-4 3.0GHz PC with 1GB RAM, and a DV camera was employed to capture video. We employ the SIFT method [11] to build the reliable correspondences between the model image and the target image. Moreover, a model image is usually acquired when the nonrigid shape contains no deformation.

In our experiments, a set of synthetic data is used to select the parameters, and the reference mesh is manually registered. The performance is evaluated by measuring the percentage of mesh vertices within two pixels of those in the reference mesh. The RBF kernel width ρ is set to 1.0, and the best regularization coefficient is found to be around 0.005 by grid searching. Similarly, the initial support is fixed to 2.0, and the annealing coefficient is 0.7.

4.2. Nonrigid Shape Recovery

We investigate the proposed nonrigid shape recovery performance on some deformable surfaces based on a piece of paper. To evaluate the effectiveness of the proposed method, the grid mesh is mapped from the model image to the input image using the recovered mapping function.

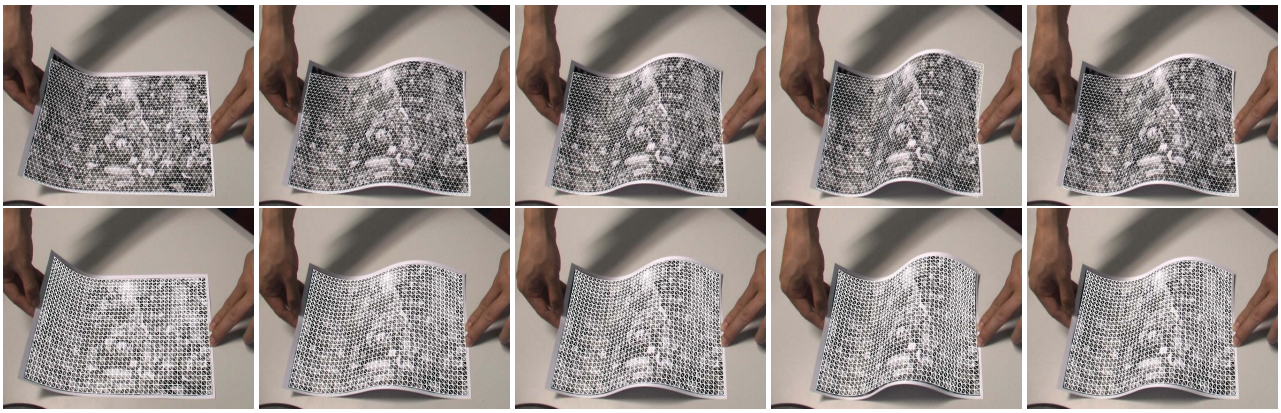

Figure 5. Recovering the paper surface with waveform deformation. The first row shows the results using the FEM-based method [24]. The second row plots the results obtained from proposed method.

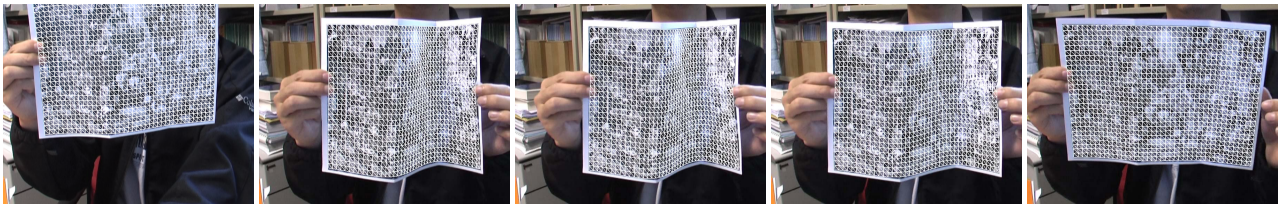

Figure 6. Recovering the sharply folded paper surface in the cluttered environment using the proposed approach.

As shown in Fig. 3, the proposed method is robust in handling large bending deformations. Moreover, we compare the proposed approach with the FEM-based method [24], whose results are illustrated in the first row. It can be clearly observed that the FEM-based approach fails in the cases with severe bending due to the oversmoothing regularization method. On the other hand, our proposed method can successfully deal with the cases by taking advantage of the Gaussian process prior on the surface deformation. We also study the nonrigid shape recovery performance in the cluttered environment, as shown in Fig. 4. Fig. 5 shows the experimental results on the waveform deformation using both the FEM-based method and our approach. We find that large registration errors occur in the boundary region using the FEM-based method. As for our proposed approach, it accurately recovers the nonrigid shape from the input image. Furthermore, we investigate the sharply folded surface deformation with the cluttered background, and plot the results in Fig. 6.

The complexity of the proposed method is determined by the order of Eqn. 9, which is equal to the total number of inlier matches. As shown in Fig. 7, we employ the proposed method to track the nonrigid object and re-texture a piece of paper as in [16, 24]. The proposed method runs around 14 frames per second on real-time video with size of 720×576, which requires about 20 iterations to achieve the convergence. The semi-implicit iterative approach [16] runs about 9 frames per second with a mesh of 120 vertices, and gradient-based method [24] runs around 18 frames per second.

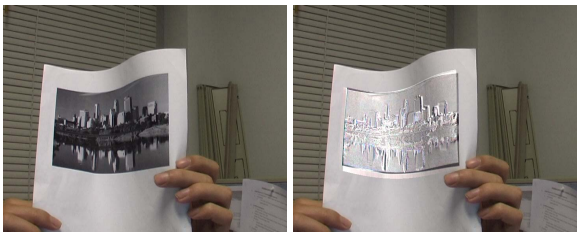

Figure 7. Re-texturing a picture on a piece of paper. The left image is the input frame. The right image is the re-texturing result.

4.3. Medical Image

We also evaluate the proposed approach for medical image registration. A pair of sagittal images [15] with size of 256×256 from two different patients are used in the experiments. The source and target images differ in both geometry and intensity. The results are plotted in Fig. 8; it can be seen that the source image is successfully registered. In comparison with the locally affine but globally smooth method [15], which takes about four minutes, our proposed method can solve the problem within half a second. Moreover, the sparse correspondences-based method can naturally handle the missing data and partial occlusion problem. As shown in Fig. 8, even with the source images in a region removed, the nonrigid shape can still be recovered. Since it is a fully automated approach, we can employ the fitting result to initialize other local methods [15] in order to further improve the registration accuracy.

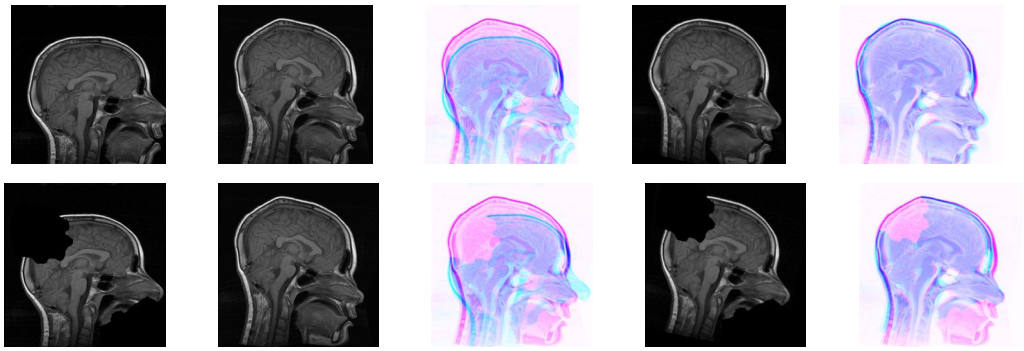

(a) Source (b) Target (c) Before (d) Registered (e) After

Figure 8. Applying the proposed method to medical image registration. A pair of sagittal images from two different patients is shown. (a,b,d) are the source, target and registered source respectively. (c) and (e) are the overlaid images before and after registration. The second row displays the synthetic example with missing data.

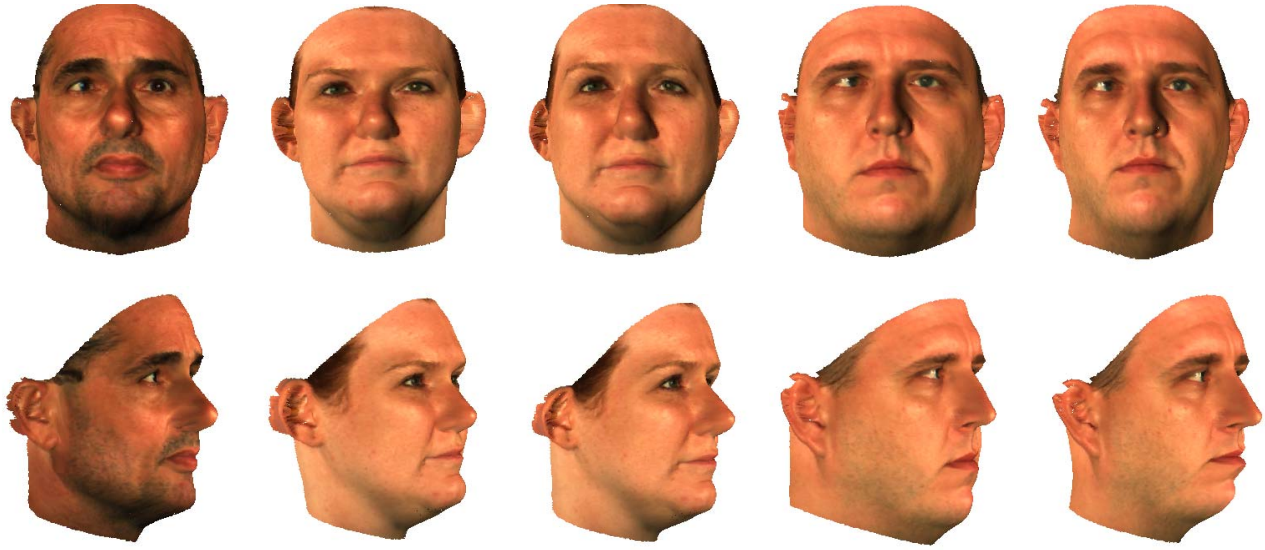

(a) Target face (b) Input female face (c) Aligned face (d) Input male face (e) Aligned face

Figure 9. Applying the proposed method to 3D face registration. (a) shows the target 3D face model. (b,d) are the two input 3D faces. (c) and (e) illustrates the results after deformation. The second row displays the rendered profile view of 3D face models in the first row.

4.4. 3D Face Registration

The proposed method can be directly applied to the 3D deformable surface registration. We employ the 3D morphable model [2] to synthesize three sample face models, as shown in Fig. 9. We randomly select 500 correspondences from over 79K points to facilitate the proposed method. Once the input face is registered using the selected matches, we transform the remaining points to the target surface by the learnt mapping function. Fig. 9 illustrates the fitting results both in frontal view and in profile view.

5. Discussions and Future Work

We have proposed a Gaussian process regression approach to nonrigid shape recovery. Compared with the FEM based methods [16, 24], the proposed method makes no assumption about the model except for a Gaussian process prior, which does not require an explicit mesh model. Moreover, the proposed method can handle severe deformations, while the FEM based methods may fail due to the over-smoothing second order regularization. It is easy to implement the proposed approach, which only involves solving a linear equation. Although the linear system of the present method is not a sparse one as in [16], experimental results indicate that the proposed approach is more efficient than the semi-implicit iterative method. This is mainly because the presented optimization scheme requires fewer iterations and the problem size is greatly reduced. Furthermore, the presented method can be directly applied to the high-dimensional data.

Although promising experimental results have validated the efficacy of the proposed approach, some limitations and future directions should be addressed. First of all, some jitter may occur due to the point matching algorithm. Second, we only employ the synthesized data to evaluate the 3D face registration. In future work, the effective feature descriptors will be introduced to deal with the jittering problem. Finally, we consider to implement the 3D feature descriptor and feature matching method described in [14] to facilitate the real-world 3D registration.

6. Conclusion

It is clear that our novel approach to nonrigid shape recovery is powerful and effective. It offers several distinct advantages over the conventional approaches. First, we propose a novel non-parametric Bayesian approach to nonrigid shape recovery. Moreover, our method can handle the large deformations without resorting to a 3D deformable surface model. Finally, our active set selection gradually decreases the noise variations, which can handle the noisy feature matching with large numbers of outliers.

Our approach has been tested in several applications, such as recovery of highly deformed shape from single images, Augmented Reality, medical image, 3D face alignment. Encouraging experimental results show that our proposed approach is both effective and promising.

Acknowledgments

The work was fully supported by the Research Grants Council Earmarked Grant (CUHK4158/08E) and the Singapore MOE AcRF Tier-1 research grant (RG67/07).

References

[1] S. Belongie, J. Malik, and J. Puzicha. Shape matching and object recognition using shape contexts. *IEEE Trans. on Pattern Analysis and Machine Intelligence*, 24(4):509–522, 2002.

[2] V. Blanz and T. Vetter. Face recognition based on fitting a 3d morphable model. *IEEE Trans. on Pattern Analysis and Machine Intelligence*, 25(9), 2003.

[3] S. Boyd and L. Vandenberghe. *Convex Optimization*. Cambridge University Press, 2004.

[4] H. Chui and A. Rangarajan. A new point matching algorithm for non-rigid registration. *Comput. Vis. and Image Underst.*, 89(2-3):114–141, 2003.

[5] O. Chum and J. Matas. Matching with prosac- progressive sample consensus. In *Proc. Conf. Computer Vision and Pattern Recognition*, volume 1, pages 220–226, 2005.

[6] S. Granger and X. Pennec. Multi-scale em-icp: A fast and robust approach for surface registration. In *Proc. European Conf. Computer Vision*, pages 418–432, 2002.

[7] C. Haili and R. Anand. A feature registration framework using mixture models. *MMBIA*, pages 190–197, 2000.

[8] S. Ilic and P. Fua. Implicit meshes for surface reconstruction. *IEEE Trans. on Pattern Analysis and Machine Intelligence*, 28(2):328–333, February 2006.

[9] B. Jian and B. C. Vemuri. A robust algorithm for point set registration using mixture of gaussians. In *ICCV*, pages 1246–1251, 2005.

[10] O. C. Keerthi, S. and D. Decoste. Building support vector machines with reduced classifier complexity. *Journal of Machine Learning Research*, 8:1–22, August 2006.

[11] D. G. Lowe. Distinctive Image Features from Scale-Invariant Keypoints. *Int'l J. Computer Vision*, 60(2):91–110, 2004.

[12] P. Meer. Robust techniques for computer vision. In M. Gerard and K. S. B., editors, *Emerging Topics in Computer Vision*. Prentice Hall, July 2004.

[13] A. Myronenko, X. Song, and M. Carreira-Perpinan. Nonrigid point set registration: Coherent point drift. In *Advances in Neural Information Processing Systems 19*. MIT Press, 2007.

[14] J. Novatnack and K. Nishino. Scale-dependent/invariant local 3d shape descriptors for fully automatic registration of multiple sets of range images. In *ECCV (3)*, pages 440–453, 2008.

[15] S. Periaswamy and H. Farid. Medical image registration with partial data. *Medical Image Analysis*, (10):452–464, 2006.

[16] J. Pilet, V. Lepetit, and P. Fua. Fast non-rigid surface detection, registration, and realistic augmentation. *Int'l J. Computer Vision*, 76(2):109–122, 2008.

[17] C. E. Rasmussen and C. K. I. Williams. *Gaussian Processes for Machine Learning*. The MIT Press, 2006.

[18] M. Salzmann, R. Hartley, and P. Fua. Convex optimization for deformable surface 3-d tracking. In *Proc. Int'l Conf. Computer Vision*, October 2007.

[19] M. Salzmann., N. Moreno, V. Lepetit, and P. Fua. Closed-form solution to non-rigid 3d surface registration. In *Proc. European Conf. on Computer Vision*, pages IV: 581–594, 2008.

[20] M. Salzmann, J. Pilet, S. Ilic, and P. Fua. Surface deformation models for nonrigid 3d shape recovery. *IEEE Trans. Pattern Anal. Mach. Intell.*, 29(8):1481–1487, 2007.

[21] R. Szeliski and J. Coughlan. Spline-based image registration. *Int. J. Comput. Vision*, 22(3):199–218, 1997.

[22] J. Zhu, S. C. Hoi, and M. R. Lyu. Real-time non-rigid shape recovery via active appearance models for augmented reality. In *Proc. European Conf. Computer Vision*, pages 186–197, 2006.

[23] J. Zhu, S. C. Hoi, Z. Xu, and M. R. Lyu. An effective approach to 3d deformable surface tracking. In *Proc. European Conf. Computer Vision*, pages III: 766–779, 2008.

[24] J. Zhu and M. R. Lyu. Progressive finite newton approach to real-time nonrigid surface detection. In *Proc. Conf. Computer Vision and Pattern Recognition*, pages 1–8, 2007.

[25] J. Zhu, M. R. Lyu, and T. S. Huang. A fast 2d shape recovery approach by fusing features and appearance. *IEEE Trans. Pattern Anal. Mach. Intell.*, 2008.